ELSEVIER

Journal of Crystal Growth 222 (2001) 202–208

JOURNAL OF CRYSTAL GROWTH

www.elsevier.nl/locate/jcrysgro

Structural defects of $Pb(Mg_{1/3}Nb_{2/3})O_3$–$PbTiO_3$ single crystals grown by a Bridgman method

Guisheng Xu*, Haosu Luo, Haiqing Xu, Zhenyi Qi, Pingchu Wang, Weizhuo Zhong, Zhiwen Yin

Laboratory of Functional Inorganic Materials, Shanghai Institute of Ceramics, Chinese Academy of Sciences, Shanghai, 201800, People's Republic of China

Received 1 November 1999; accepted 2 October 2000
Communicated by L.F. Schneemeyer

Abstract

The types, formation mechanism and suppressing approaches of structural defects in PMNT crystals grown by a Bridgman method were investigated in this paper. The structural defects include composition non-uniformity, scattering particles, pores, negative crystal structures, cellular structures, fissure structures and point defects. They are formed due to one or several of the following: composition deviation, incomplete melting and diffusion, high-temperature volatilization, temperature fluctuation and instability of the position and shape of growth interfaces. On understanding the formation mechanism of structural defects, one can restrain them by means of adjusting stoichiometry of starting materials, using PMNT crystal bulks, suppressing composition volatilization and modifying growth parameters.

PACS: 81.10.Fq; 77.84.−s; 77.84.Dy

Keywords: PMNT; Piezocrystals; Structural defects; Crystal perfection; Bridgman method

1. Introduction

Perovskite relaxor-based ferroelectric single crystals $Pb(Mg_{1/3}Nb_{2/3})O_3$–$PbTiO_3$ (PMNT), $Pb(Zn_{1/3}Nb_{2/3})O_3$–$PbTiO_3$ (PZNT), and $Pb(Sc_{1/2}Nb_{1/2})O_3$–$PbTiO_3$ (PSNT) exhibit excellent piezoelectric properties, which surpass largely those available from the conventional PZT piezoelectric ceramics [1–5]. They have attracted great attentions for their potential and important applications in medical ultrasonic transducers, sonars and solid actuators. Their domain structures have been observed [5,6], and some explanations, for example, field induced R–T phase transition [2,7] and polarization rotation [8], have been put forward for their giant piezoelectric response achieved on the domain engineered (0 0 1) cuts of rhombohedral crystals. On the other hand, some progresses in the growth of these crystals have been achieved in recent years. PZNT

*Corresponding author. Present address: Shanghai Institute of Ceramics, Chinese Academy of Sciences, Jiading District, Shanghai 201800, People's Republic of China. Fax: +86-021-59927184.

E-mail address: gshxu@hotmail.com (G. Xu).

0022-0248/01/$ - see front matter
PII: S0022-0248(00)00917-9

and PMNT crystals grown by conventional PbO flux methods reached the size of 20 mm and 15 mm respectively [2,9]. A larger PZNT crystal up to $43 \times 42 \times 40\,mm^3$ was grown by a modified PbO flux method, in which local temperature gradient was enhanced by oxygen gas transported in pipes and concentrated nucleation reduced to a certain degree [10]. In order to strengthen further the control of spontaneous nucleation, a vertical Bridgman method adding PbO flux (occupying 55 mol% in total PZNT–PbO solution) was adopted to grow PZNT crystals, with the boules reaching the size of $\phi 40\,mm \times 20\,mm$ [11].

However up to now, only a few of crystals grown by above methods could reach the size of $40 \times 40 \times 40\,mm^3$ by chance, which was the demand of transducer probes for crystal size, and the growth rate was slow too. It is necessary to seek a more proper method to scale up the growth of these valuable piezocrystals. A Bridgman method was adopted to grow PMNT crystals in this paper. This method had some obvious advantages compared to aforementioned methods. First, crystal seeds were adopted for the first time in this method. The crystal seeds had a key effect on restraining spontaneous nucleation and parasitic growth. Second, PMNT melt without PbO flux was directly used, which would be favorable for a rapid growth and the control of supercooling (or supersaturation) and the solid–liquid interfaces. By now, as large as $\phi 40\,mm \times 80\,mm$ PMNT crystals can be repeatedly obtained by this Bridgman method and the problems in crystal size and growth rate have been solved satisfactorily [5,12]. The issues of crystal perfection or defects, which includes composition nonuniformity, scattering particles, pores, negative crystal structures, cellular structures, fissure structures and point defects, and the approaches to enhance crystal perfection and the piezoelectric properties will be discussed in the paper.

2. Experimental procedure

The melting points of PMNT were measured by NETZSCH-STA492 thermal analyzer. The samples were placed in crucibles with lids (semi-sealed condition) and measured under air atmosphere. A Bridgman method was adopted to grow PMNT single crystals. The starting materials were highly pure powders (99.99%) of PbO, MgO, TiO_2 and Nb_2O_5 with the PMN to PT ratio of 76/24–65/35, or PMNT crystal bulks obtained from boules. The crystal boules grown by using powder starting materials at first time were cut into three parts, i.e. crystal seed, crystal bulk and impurity, which was formed by segregation and located atop the boules. The crystal bulk was then used as "starting materials" at the second growth and called as crystal bulk sample. After platinum crucibles were charged by powder or crystal bulk samples, they were put in furnaces with two temperature chambers. By means of controlling the temperature and descendant rate of the crucibles, PMNT single crystals were obtained.

PMNT crystals were processed to polished plates for the observation of crystal defects and domain configurations under optical microscope, scanning electron microscope (SEM) and atomic force microscope (AFM). The plates coated with Cr and Au electrodes were poled under an electric field of 10 kV/cm. Ferroelectric hysteresis loops were tested by an RT66A standard ferroelectric test system and dielectric properties measured by an HP4192A impedance analyzer. The piezoelectric constant d_{33} was measured with a quasi-static d_{33} meter of Berlincourt type. The thickness mode (k_t) and longitudinal bar mode (k_{33}) electromechanical coupling factors on $\{0\,0\,1\}$ cuts were calculated from resonance and antiresonance frequencies.

3. Results and discussion

3.1. Composition nonuniformity

Table 1 shows the dielectric and piezoelectric properties of PMNT crystals. The variations in dielectric constant ε and Curie temperature (T_c) or rhombohedral-tetragonal phase transition temperature (T_{R-T}) amongst different points of a plate are obviously caused by composition nonuniformity. In fact, this composition fluctuation can also be reflected by the nonuniform distribution of domains. Fig. 1 illustrates the coexistence of two types of domain configuration, broader and

Table 1
The dielectric and piezoelectric properties of PMNT single crystals with (0 0 1) cut types[a]

Sample number	Composition	ε	$\tan\delta$ (%)	k_t	k_{33}	d_{33} (pcN^{-1})	T_c (°C)	T_{R-T} (°C)
1-a	76/24	3450–3900	0.4–0.9	0.55		850–940	107–111	
2-a	76/24	2890–3550	0.6–1.1	0.54		890–1000	108–113	
3-b	76/24	3450–3510	0.6–0.7	0.57		980–1010	110	
4-a	67/33	4470–4960	0.4–0.9	0.61	0.90	2000–2300	150–154	54–59
5-a	67/33	5450–5820	0.3–0.6	0.62	0.91	2400–2800	146–149	75–82
6-b	67/33	5555–5620	0.5–0.6	0.63	0.93	2980–3100	151	51–52

[a] a – samples with metal oxides as starting materials.
b – samples with crystal bulks as starting materials.

Fig. 1. Nonuniform distribution of domains in PMNT 67/33 crystals under polarizing microscope.

narrower strips, in a PMNT 67/33 crystal near MPB.

Due to the composition complexity and the segregation of four-component PMNT solid solution system, there is composition nonuniformity among different plates. Generally, it is slight, near or lower than the error limits and cannot be measured precisely by X-ray fluorescence spectrometry. But there are substantial differences of various PMNT compositions in melting points, from PMN~1320°C, PMNT76/24~1289°C, PMNT 67/33~1280°C to PT~1255°C, which suggests that macro segregation exists though it is slight. XRD data of different plates from a boule also indicate that crystal structure moves to Ti-rich field of PMN-PT pseudo-binary system from the bottom up. The variation of dielectric and piezoelectric properties in various plates may be mainly ascribed to above macrosegregation.

It was found that, under the same growth conditions, using PMNT crystal bulks as starting materials could achieve a better composition or property uniformity than using oxide powders (Table 1). In fact, when stoichiometric oxide powders were used as starting materials, some red PbO crystalline grains frequently existed in the form of segregation materials near crucible walls, especially in the places near crystal seeds. This phenomenon might arise from the relatively high density of PbO. However, PbO segregation materials disappeared while crystal bulks were used.

3.2. Scattering particles

Scattering particles can be observed under crossed polarizing microscope as interference color bands (Fig. 2). They are tiny solid or gas inclusions smaller than 0.01 mm. Incomplete melting of starting materials, whose melting points changed in the range from 886°C of PbO to 2830°C of MgO, might exist at growth temperature of 1390°C (about 100°C higher than the melting point of PMNT crystals) and generated some solid-state scattering particles. Therefore, scattering particles could be reduced or eliminated by raising further growth temperature or prolonging soaking time. However, other scattering particles were formed by composition deviation. The excess components could form solid scattering particles whereas the deficient components could form microgas ones or vacancy mass. Hence, it was necessary to adjust stoichiometry of starting materials.

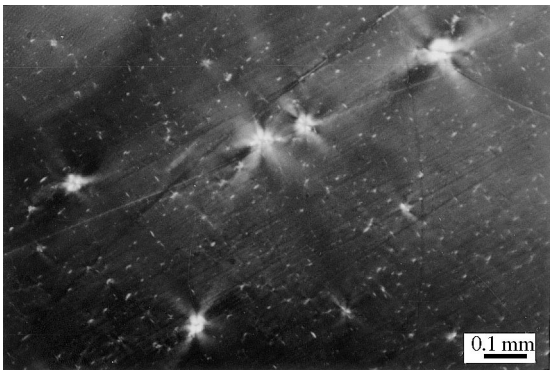

Fig. 2. Scattering particles in PMNT 76/24 crystals under crossed polarizing microscope.

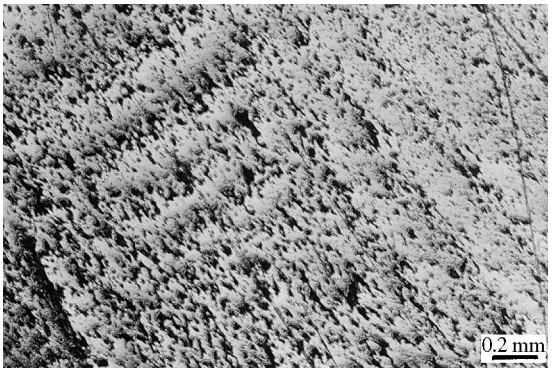

Fig. 3. Pores in PMNT 67/33 crystals under polarizing microscope.

3.3. Pores

Tiny gas inclusions or pores with the size of 1~3 μm are the predominant macro defects in PMNT crystals. The gas derives from the volatilization of PMNT. By increasing growth temperature or slowing down growth rate, the bubbles would shift faster or diffuse more efficiently in the melts and the nucleation of bubbles would become difficult so that the pores become less.

Sometimes, growth rate surpassing the descending rate of crucibles, or growth acceleration, became a main reason for pores especially when crystal growth came into later stages. In this case, the number of pores increased along the direction from the bottom up and a number of pores near the top end of boules were arranged along 71° (or 109°) domain walls (Fig. 3). These pores can be reduced largely by raising growth temperature or decreasing the descending rate of crucibles gradually during the period of crystal growth, as confirmed in our experiments.

3.4. Negative crystal structures

Negative crystal structures, which have regular faces and the same crystallographic orientation as that of the crystals themselves, can be observed by naked eyes or under optical microscope. They appear in two kinds of size, the big one being about 1.0 mm (Fig. 4) and the small one about 0.02 mm, and they are red mixture of PbO and

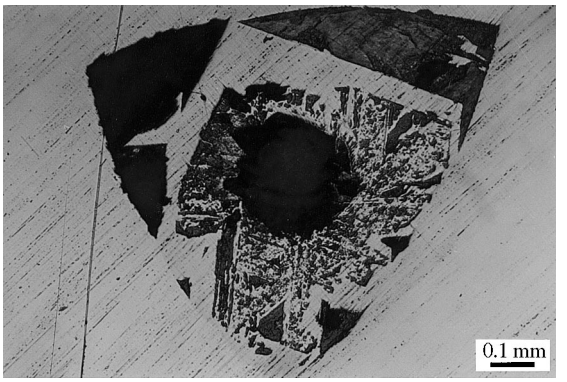

Fig. 4. Negative crystal structures on a {1 1 1} plate of PMNT 76/24 crystal under polarizing microscope.

pyrochlore. The sudden temperature fluctuation in the range of 1°C sometimes occurred due to the instability of heating elements, ambient temperature and compositional volatilization. In this case, rapid constitutional supercooling might take place and some of melts be surrounded by crystals. These melts then froze gradually at the inner of crystals and formed negative crystals in the subsequent cooling stage. Therefore, the negative crystal structures can be reduced or eliminated by lessening the temperature fluctuation.

3.5. Cellular structures

Cellular structures, which consist of yellowish PMNT crystals in little flanges and red PbO flux in straight lines, mainly develop on the upper part of boules while some PbO as flux are added. The PbO flux distributes along {0 0 1}, thus, the related

cellular structures take the shape of right delta along [1 1 0] on {1 1 1} plates (Fig. 5) or right quadrangle on {0 0 1} plates. It is interesting to note that there are secondary small deltas within primary big deltas.

The cellular structures originated from the decreasing of temperature gradient and constitutional supercooling caused by the shifting down and becoming concave of solid–liquid interfaces due to the decreasing of freezing temperature of PMNT–PbO solution. Therefore, it is more difficult to control crystal perfection in flux-Bridgman methods, though the growth temperature dropped down in the case.

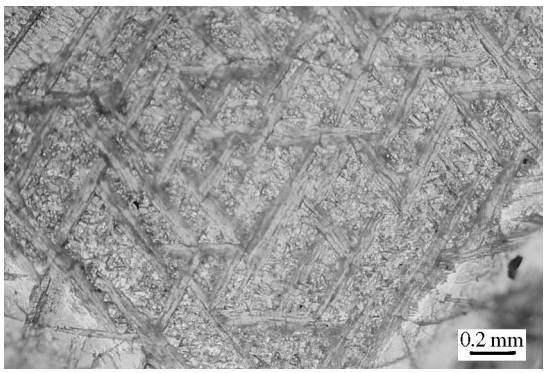

Fig. 5. Cellular structures taking the shape of delta along [1 1 0] on a {1 1 1} plate.

3.6. Fissure structures

Fissure structures in PMNT crystals can be observed by naked eyes or under atomic force microscope (Fig. 6), which mainly appear near the top end of boules and develop along {0 0 1}. The existence of {0 0 1} fissures in PMNT crystals is not of necessity from the view of crystallochemistry since the linking force of particles is still strong along [0 0 1] in perovskite structure. On the other hand, the phase transition in solid state is not an important reason for the formation of fissure structures either, which was confirmed by annealing experiments of PMNT crystals. Therefore, the appearance of {0 0 1} fissure structures can be mainly ascribed to the effect of thermal stress and structure stress generated by the changes in axial and radial temperature gradient while the position and shape of solid–liquid interfaces change during the growth process. When growth interfaces shifted up, the crystals newly formed

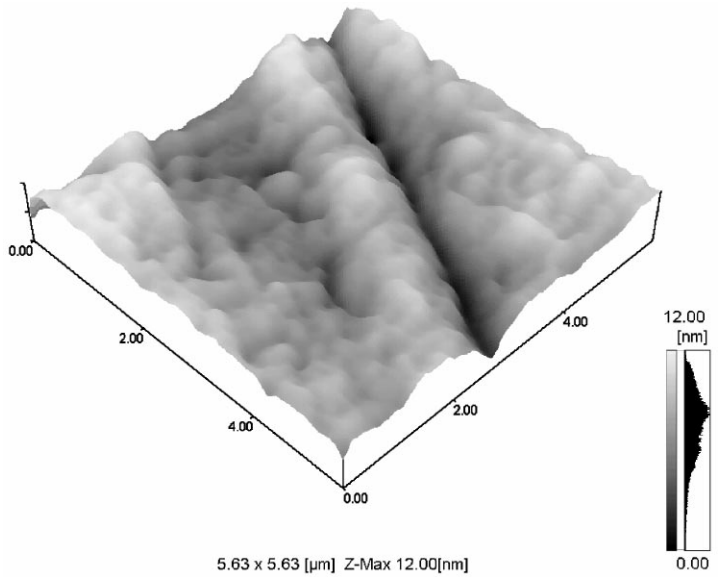

Fig. 6. Micro fissure structures in PMNT 67/33 crystals under atomic force microscope.

would pass through the region with the largest axial temperature gradient in furnaces. Meanwhile, more convex growth interfaces would introduce larger radial temperature gradient. The defects in company with the shifting up of growth interfaces promoted further the formation of fissure structures. On the other hand, solid–liquid interfaces, when adding PbO as flux, readily shifted down and changed from flat to concave, giving rise to the increase of thermal stress and the formation of fissure structures, which were frequently accompanied by aforementioned cellular structures. Therefore, controlling the position and shape of growth interfaces is not only a key for reducing pores and cellular structures, but also a key for eliminating fissure structures. In practice, these defects in PMNT single crystals are greatly reduced by maintaining the stability of growth interfaces.

3.7. Point defects

Experimental results demonstrate that there are point defects in PMNT crystals. Some as-grown crystals with abnormal gray colors can recover normal yellowish colors after undergoing high temperature annealing in air or being used as crystal seeds. This indicates the existence of oxygen vacancies, which can be partly compensated in oxygen-rich atmosphere. It is possible that there are a few of oxygen vacancies as well in the crystals with normal colors since the differences of both cases are merely in the amount of oxygen expelled out from starting oxides or PMNT melts. Sometimes, free charge carriers or electric current can be observed while poling, which also demonstrates the existence of point defects in PMNT plates due to the association of free charge carriers and point defects.

The space charge field derived from point defects has "pinning-up effectiveness" on domains, making polarization switching difficult and piezoelectric properties poor. The abrupt changes in values of d_{33} in small regions of 2–3 mm^2 for some PMNT plates is more related to point defects than composition fluctuation. It is also found that the values of piezoelectric constant d_{33} in some plates can be enhanced from 1000 to 2200 pC/N after the poling electric field changes from 10 to 20 kV/cm. This can be ascribed to the effectiveness of removing polarization "pinning-up" under high poling field.

Point defects in crystals can form an interior bias field, which is shown by left–right asymmetry of ferroelectric hysteresis loops. For a PMNT 67/33 sample at 20°C, the coercive fields in positive (E_c^+) and negative directions (E_c^-) are 4.266 and −3.368 kV/cm, respectively. Thus, the interior bias field E_i is calculated as 0.449 kV/cm. The test on hysteresis loops also illustrates that the values of E_i tend to decrease with the uprising of temperature (Fig. 7). When temperature rise up, the thermal movement of point defects becomes faster and the spontaneous polarization drops down as well, thereby giving rise to the falling of E_i. The irregular variation of E_i in Fig. 7 in the range of 40–80°C, which corresponds to T_{R-T}, may result from rhombohedral-to-tetragonal phase transition. As we know, the direction of E_i is parallel to that of spontaneous polarization, therefore, E_i changes with spontaneous polarization, which varies remarkably during diffuse R–T phase transition.

4. Conclusions

Owing to the composition complexity, segregation and high-temperature volatilization of PMN–PT system, PMNT crystals grown by the Bridg-

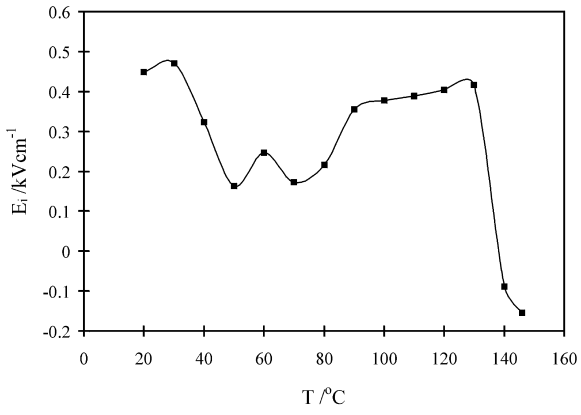

Fig. 7. The temperature dependence of the values of bias field E_i in a sample of PMNT 67/33 crystal.

man methods may contain some structural defects, which include composition nonuniformity, scattering particles, pores, negative crystal structures, cellular structures, fissure structures and point defects. These defects closely affect the crystal perfection and pizeoelectric properties. Based on the formation mechanism of above defects, the main approaches of reducing or eliminating them are proposed as follows: (i) adjusting stoichiometry of starting materials; (ii) suppressing composition volatilization; (iii) raising growth temperature; (iv) prolonging soaking time; (v) lowering the descending rate of crucibles and (vi) controlling on the interface stability in position and shape.

Acknowledgements

This research has been supported by National Natural Science Foundation of China (Grant Nos. 59995520 and 59872048), Chinese Academy of Sciences (Grant No. KY951-A1-205-03), Shanghai Municipal Government (Grant No. 99XD14024) and General Electric Company, USA.

References

[1] R.E. Service, Science 275 (1997) 1878.
[2] S.E. Park, T.R. Shrout, J. Appl. Phys. 82 (4) (1997) 1804.
[3] Y. Yamashita, S. Shimanuki, Mater. Res. Bull. 31 (7) (1996) 887.
[4] M. Dong, Z.G. Ye, J. Crystal Growth 209 (2000) 81.
[5] G.S. Xu, H.S. Luo, W.Z. Zhong, Z.W. Yin, H.Q. Xu, Z.Y. Qi, K. Liu, Sci. China Ser. E 42 (5) (1999) 521.
[6] Z.G. Ye, M. Dong, J. Appl. Phys. 87 (5) (2000) 2312.
[7] M.K. Durbin, E.W. Jacobs, J.C. Hicks, S.E. Park, Appl. Phys. Lett. 74 (1999) 2848.
[8] H. Fu, R.E. Cohen, Nature 403 (2000) 281.
[9] T.R. Shrout, Z.P. Chang, N. Kim, S. Markgraf, Ferroelect. Lett. 12 (1990) 63.
[10] T. Kobayashi, S. Shimanuki, S. Saitoh, Y. Yamashita, Jpn. J. Appl. Phys. 36 (1997) 272.
[11] K. Harada, Y. Hosono, S. Saitoh, Y. Yamashita, Jpn. J. Appl. Phys. 39 (5B) (2000) 3117.
[12] G.S. Xu, H.S. Luo, P.C. Wang, H.Q. Xu, Z.W. Yin, Chinese Sci. Bull. 45 (6) (2000) 491.